



Pre-Rodinia supercontinent Nuna shaping up: A global synthesis with new paleomagnetic results from North China

Shihong Zhang^{a,*}, Zheng-Xiang Li^{b,c}, David A.D. Evans^d, Huaichun Wu^a, Haiyan Li^a, Jin Dong^a

^a State Key Laboratory of Biogeology and Environmental Geology, China University of Geosciences, Beijing, 100083, China

^b Department of Applied Geology, ARC Centre of Excellence for Core to Crust Fluid Systems (CCFS), Curtin University, GPO Box U1987, Perth, WA, Australia

^c Department of Applied Geology, The Institute for Geoscience Research (TIGeR), Curtin University, GPO Box U1987, Perth, WA, Australia

^d Department of Geology and Geophysics, Yale University, New Haven, CT 06520-8109, USA

ARTICLE INFO

Article history:

Received 23 June 2012

Received in revised form

20 July 2012

Accepted 21 July 2012

Editor: T.M. Harrison

Keywords:

paleomagnetism
Xiong'er Group
North China Block
Nuna
supercontinent
reconstruction

ABSTRACT

The existence of a pre-Rodinia Precambrian supercontinent, variously called Nuna or Columbia, has been widely speculated in the past decade, but the precise timing of its existence and its configuration have been uncertain due to the lack of unequivocal paleomagnetic and geological constraints. Here we report high-quality paleomagnetic results from the well dated ~1780 Ma Xiong'er Group in southern North China Block (NCB). A total of 110 paleomagnetic samples from 14 sites were collected and subjected to stepwise thermal demagnetization. After removing a low temperature component (CL) of viscous magnetic remanence acquired in recent geomagnetic field, a high temperature component (CH), carried by hematite and magnetite in redbeds and volcanic samples, has been isolated. It gives a mean direction of ($D=18.4^\circ$, $I=-3.7^\circ$, $\alpha_{95}=7.6^\circ$, $N=14$) after bedding correction, and a corresponding paleomagnetic pole at 50.2°N , 263.0°E ($A_{95}=4.5^\circ$). The CH passed a reversal test and was interpreted as a primary remanence. This new pole plus three other high-quality poles from the NCB that have been more precisely dated at 1769 ± 3 Ma, $1560\text{--}1440$ Ma and 1437 ± 21 Ma define a 1780–1440 Ma apparent polar wander path (APWP) for the NCB. This, together with an update of global high quality paleomagnetic dataset, allows us to demonstrate that the pre-Rodinia supercontinent Nuna likely existed at least between ~1780 Ma and ~1400 Ma. Our paleomagnetism-based global reconstruction, for the first time, quantitatively assembles all major cratons together; it encompasses previously proposed regional links including the SAMBA connection between Baltica, Amazonia and Western Africa (Johansson, 2009), connections between Laurentia, Baltica and Siberia at the core of Nuna (Evans and Mitchell, 2011), the proto-SWEAT connection between Laurentia, East Antarctica and Australian blocks (Payne et al., 2009), and the NCB–India connection (Zhao et al., 2011).

© 2012 Elsevier B.V. All rights reserved.

1. Introduction

Although it has long been speculated that the Earth's evolution may have been dominated by cycles of supercontinent assembly and breakup (e.g., Nance et al., 1988), our understanding of past supercontinents has mainly been limited to the last 1000 Ma, with more confidence being placed on the history of the ca. 320–180 Ma supercontinent Pangea (Veevers, 2004) than the ca. 900–700 Ma supercontinent Rodinia (Li et al., 2008a). Our knowledge of an even older supercontinent, possibly formed by global ca. 1800 Ma orogenic events and variably named Nuna (Hoffman, 1997) or Columbia (Rogers and Santosh, 2002; Zhao et al., 2002; Zhao G. et al., 2004), has been more tenuous, and early papers were mostly based on intercontinental geological correlations that are intrinsically non-

unique. Early attempts of paleomagnetically examining Nuna-related continental reconstructions (e.g. Idrum and Giddings, 1995; Payne et al., 2009; Wu et al., 2005) were hampered by the lack of high-quality paleomagnetic results, or merely regional rather than global considerations. Evans and Mitchell (2011) provided a recent update on the assembly and breakup of the centre of Nuna, between Laurentia, Baltica and Siberia. Here we use new paleomagnetic results from North China, as well as recent results from Australia, India, and Amazonia, to examine the positions of these continental blocks in Nuna. Together with the proposed Laurentia–Baltica–Siberia connection (Evans and Mitchell, 2011), we are now able to present a geologically and paleomagnetically viable configuration for the bulk of Nuna.

2. New paleomagnetic results from North China

2.1. Geological background

The North China Block (NCB) has an Archean to Paleoproterozoic metamorphic basement, covered by post-1.85 Ga, little-deformed

* Corresponding author: State Key Laboratory of Biogeology and Environmental Geology, China University of Geosciences, Beijing 100083, China, Tel.: +86 10 82322257; fax: +86 10 82321983.

E-mail address: shzhang@cugb.edu.cn (S. Zhang).

sedimentary and volcanic successions that are amenable to paleomagnetic study (e.g. Zhang et al., 2006). Recently available high-precision U–Pb zircon ages for the volcanic units and tuff beds within the sedimentary units (Li et al., 2010; Su et al., 2008, 2010) provide the first precise age constraints on paleomagnetic results obtained from these successions, enabling us to use those results for quantitative global paleogeographic reconstructions.

Our new paleomagnetic investigation was carried out on the well-dated Xiong'er Group, which unconformably overlies the Archean and Paleoproterozoic basement rocks of the NCB. It is found in southern Shanxi Province and western Henan Province, with an outcropping area of $\sim 60,000$ km² (Fig. 1). It consists mainly of andesites and basaltic andesites, with minor dacites, rhyolites and red mudstones (He et al., 2009). Volcanic strata of the Xiong'er Group are traditionally classified into three parts: the Xushan Formation at the bottom, the Jidanping Formation in the middle, and the Majiahe Formation at the top. However, this subdivision was mainly based on petrological compositions and has been challenged by recent geochronological work (He et al., 2009). The Xushan Formation and the Majiahe Formation have similar petrological compositions. They both are dominated by basaltic andesites and andesites, but the Majiahe Formation contains more sedimentary red-beds. Zircon U–Pb ages of the volcanic rocks from these two formations are both ~ 1780 Ma, indistinguishable within uncertainties (Fig. 1b). They may represent rapid magmatic activity in the south margin of the NCB in late Paleoproterozoic, slightly older than the Taihang dyke swarm in the interior of this craton (ca. 1770 Ma, Halls et al., 2000; Wang et al., 2004).

Age constraints for the Jidanping Formation are more complex. The Jidanping Formation contains fewer basaltic rocks but more dacites and rhyolites and subvolcanic rocks than the Xushan and Majiahe formations. Some volcanic rocks of the Jidanping Formation gave the same ages within errors as the Xushan and Majiahe formations, but others gave ages as young as 1450 Ma (He et al., 2009), suggesting that the lithostratigraphically defined Jidanping Formation has a wide range of ages.

Our paleomagnetic sampling was carried out for the Xushan and Majiahe formations in the Waifang Mountain region ($\sim 33^{\circ}57'N$, $\sim 112^{\circ}27'E$, Fig. 1b), because these formations not only have tight age constraints of ca. 1780 Ma, they are also better outcropped and more fresh in that area. Outcrops without clear geological contact and concrete paleo-horizontal markers, such as those in the Jidanping Formation, were not considered in this study. A total of 110 oriented core samples were obtained from 13 sites in dark-gray or purple-gray basaltic andesites or andesites, and one site in purple mudstones of the Majiahe Formation. They were oriented using a magnetic compass, combined with a sun compass when possible. Orientation differences between the two devices are within $\pm 1^{\circ}$ in most cases, and the differences are less than $\pm 3^{\circ}$ for all samples. The strata tilt is gentle; most sites have dips of 5–20 $^{\circ}$ toward the southwest.

2.2. Experimental condition

All samples were cut into 22-mm-long specimens and subjected to stepwise thermal demagnetization. Remanence measurements were made with an AGICO JR-6A spinner magnetometer and demagnetization was made using an ASC TD-48 furnace in 5–20 $^{\circ}C$ steps up to 685 $^{\circ}C$, or until the remanence became too weak to measure. The instruments in the paleomagnetism laboratory of China University of Geosciences (Beijing) are housed in room-size Helmholtz coils with a low magnetic field of ~ 200 nT in the sample loading region. The internal residual field in the furnace is lower than 10 nT. During the experiments, samples were further protected from magnetic contamination by μ -metal shielding. Magnetic hysteresis parameters (i.e., saturation magnetization, M_s , saturation remanence, M_{rs} , coercive force, H_c , and coercivity of remanence, H_{cr}) were measured for representative samples using an alternating gradient magnetometer (MicroMag 2900). The magnetic field was cycled between ± 1.8 T for each sample. M_s , M_{rs} , and H_c were determined after correction for the paramagnetic contribution. H_{cr} was obtained when each sample was

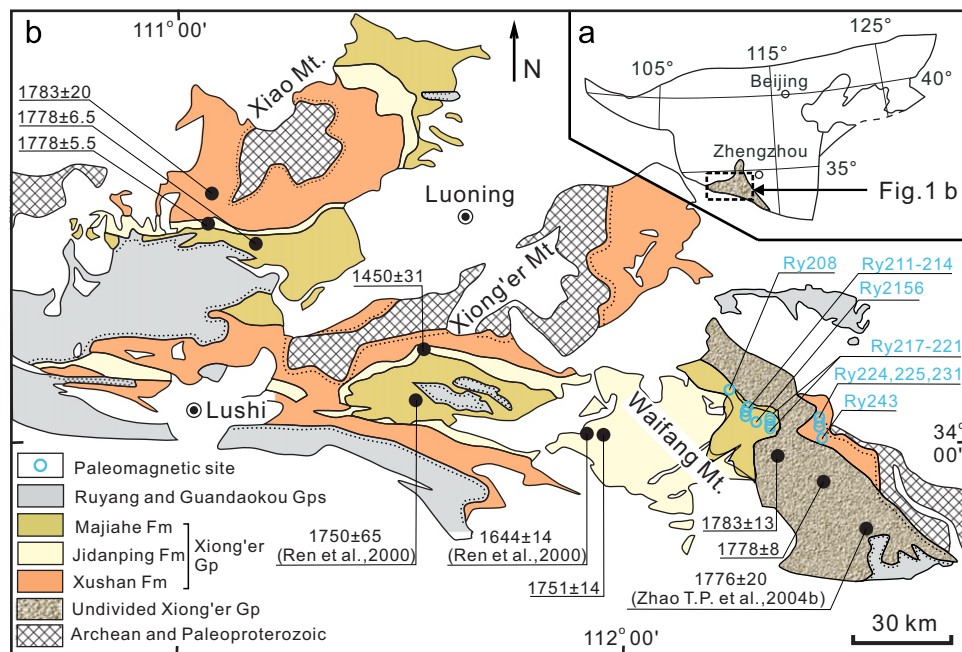


Fig. 1. (a) Tectonic outline of the North China Block (NCB). (b) Paleomagnetic and geochronological sites, and distribution and subdivision of the Xiong'er Group. Ages are in Ma, those without references are cited in He et al. (2009) (Ren et al., 2000; Zhao T.P. et al., 2004).

demagnetized in a stepwise back-field. Magnetic components were calculated using principal-component analysis (Kirschvink, 1980) for each sample. Statistics on the distribution of the directions were analyzed using Fisher statistics (Fisher, 1953).

2.3. Paleomagnetic results

The natural remanent magnetization (NRM) intensities of the volcanic samples are in the range of 30–800 mA/m, while those of the sedimentary samples (red-beds) range from 10 to 20 mA/m.

After the removal of a stray viscous magnetization, two magnetic components were identified in most samples (Fig. 2). A lower-temperature component CL was often found at the temperature range of 200–500 °C. Its in situ mean direction is close to that of the present local geomagnetic field (Fig. 3a and c), suggesting an origin of viscous magnetization acquired in recent times. A higher-temperature component CH is well defined, generally above 540 °C. The high unblocking temperatures of component CH strongly suggest that the main magnetic carriers are magnetite and hematite in the volcanic rocks, and hematite in the

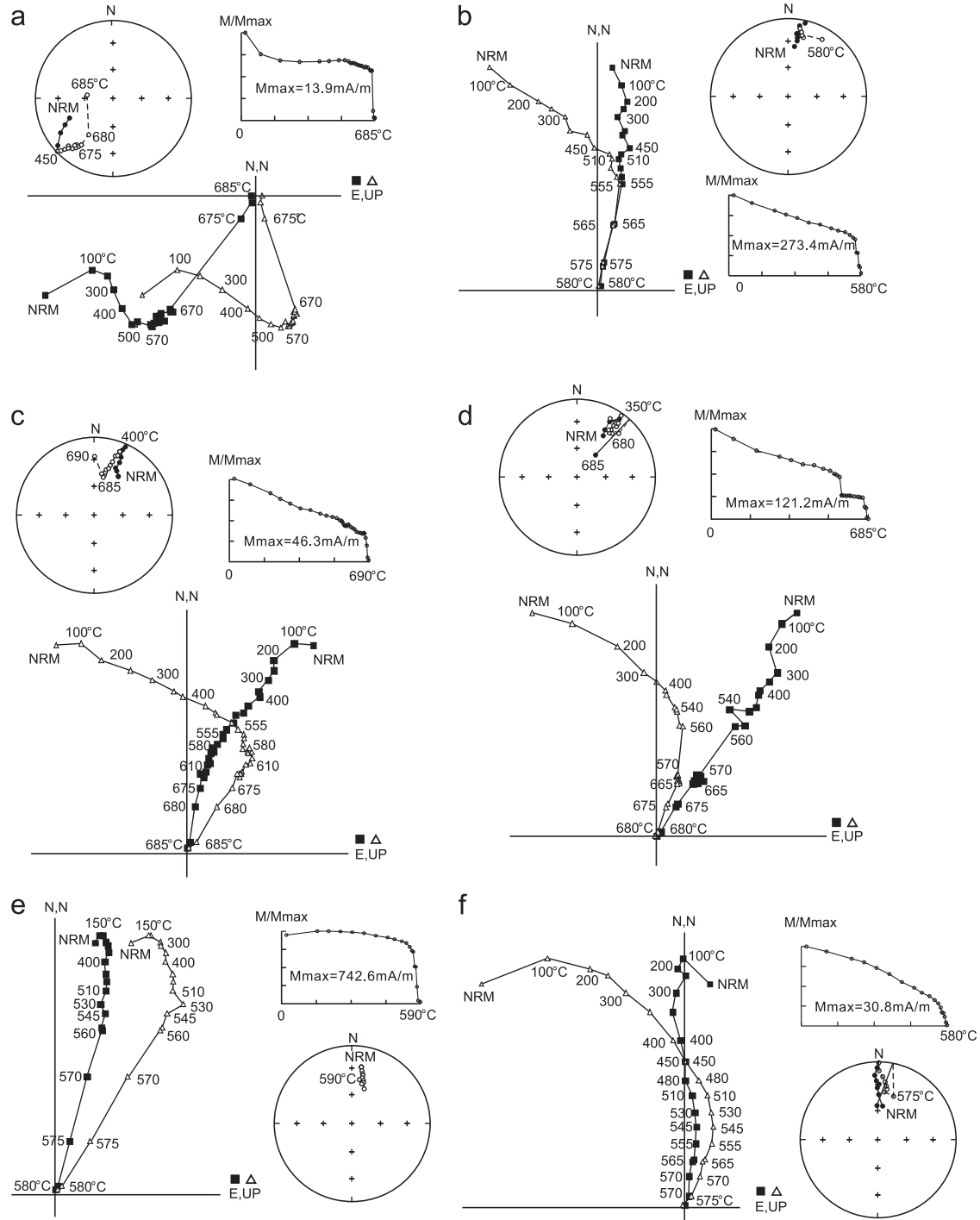


Fig. 2. Orthogonal vector plots showing the results of stepwise demagnetization of representative samples for redbeds (RY208E) and volcanic rocks (all others) of the Xiong'er Group. In orthogonal vector plots, closed square (open triangle) symbols represent projections on the horizontal (vertical) plane. NRM, Natural Remanent Magnetization. In stereoplots, closed (open) symbols represent positive (negative) inclinations.

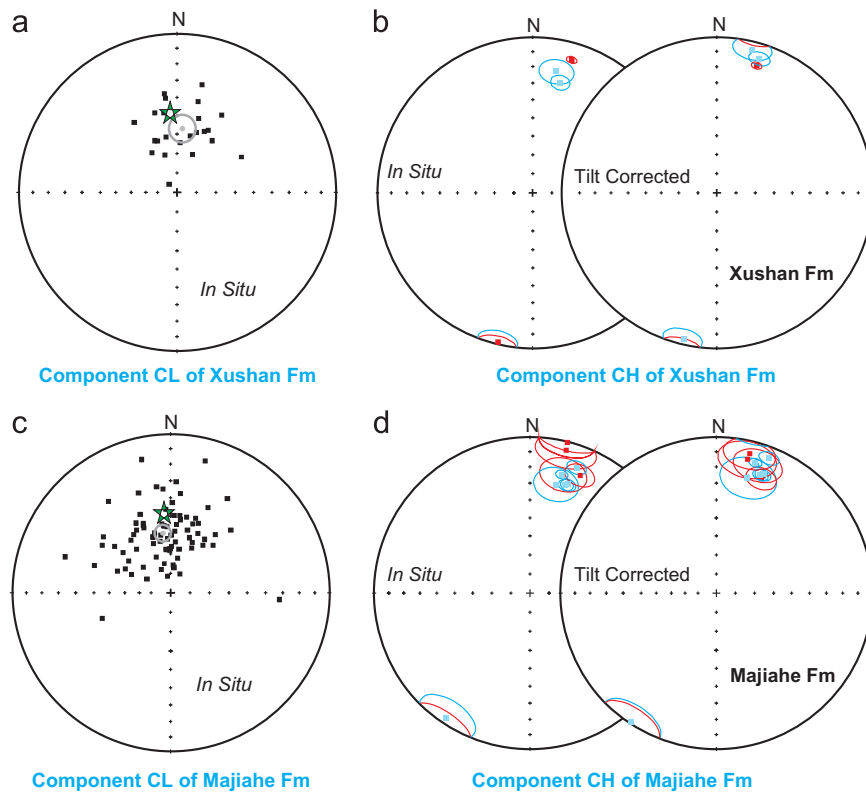


Fig. 3. Equal area projections showing paleomagnetic directions obtained from the Xiong'er Group. (a, c) Component CL from the Xushan and Majiahe formations respectively, all plotted in situ, gray dots with 95% confidence circles being mean direction at sample level, stars showing the present geomagnetic field direction. (b, d) Site mean paleomagnetic directions and their 95% circles of confidence of the high-temperature component CH from the Xushan and Majiahe formations, respectively. Red (blue) symbols represent positive (negative) inclinations.

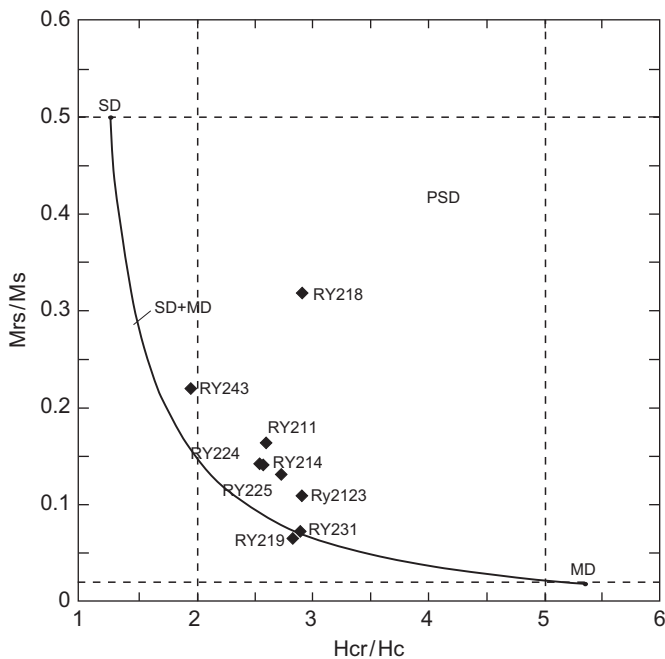


Fig. 4. Day plot for representative volcanic rock samples. Domain boundaries and the SD+MD matrix line are after Dunlop (2002). SD, single domain; PSD, pseudo-single domain; MD, multidomain; Ms, saturation magnetization; Mrs, saturation remanence; Hc, coercive force; Hcr, coercivity of remanence.

redbeds. Hysteresis results indicate that the magnetite grains are pseudo-single domain (PSD) particles in volcanic rocks (Fig. 4). Component CH points either to north–northeast or south–southwest

with shallow inclinations (Fig. 3b and d). Its mean direction on sample level after bedding tilt correction is $Ds/Is=15.6^\circ/-1.6^\circ$ ($n=27$, $a_{95}=4.4^\circ$) for the Xushan Formation, and $Ds/Is=19.5^\circ/-3.3^\circ$ ($n=76$, $a_{95}=4.1^\circ$) for the Majiahe Formation. The mean directions on site level are similar, $Ds/Is=15.5^\circ/0.8^\circ$ ($N=4$, $a_{95}=13.1^\circ$) for the Xushan Formation, and $Ds/Is=19.6^\circ/-5.5^\circ$ ($N=10$, $a_{95}=10.0^\circ$) for the Majiahe Formation, indistinguishable between the two formations within errors (Table 1). Within the Majiahe Formation, the direction of component CH from the redbed site has the opposite polarity to that of all the lava sites. In the Xushan Formation, component CH remanence of opposite polarities has been observed from different lava beds, passing the reversals test of McFadden and McElhinny (1990) at 95% confidence level ($\gamma_0=6.6^\circ < \gamma_{critical}=8.3^\circ$, classification B). We interpret component CH as a remanence acquired by the volcanic rocks during cooling and by the sedimentary rocks during deposition or early diagenesis.

We calculated the VGPs corresponding to each site-mean direction first, and then averaged these VGPs to determine the paleomagnetic pole and its error A_{95} . As listed in Table 1, the mean pole position for the Xushan Formation falls at $53.4^\circ N$, $265.9^\circ E$ ($A_{95}=7.0^\circ$), and mean-pole for the Majiahe Formation falls at $48.8^\circ N$, $262.0^\circ E$ ($A_{95}=5.9^\circ$). The two poles overlap each other. Since the Majiahe and Xushan formations are indistinguishable in age, we averaged the VGPs of all 14 sites and obtained an overall mean-pole position at $50.2^\circ N$, $263.0^\circ E$ ($A_{95}=4.5^\circ$) for the ~ 1780 Ga Xiong'er Group (Table 1). This pole does not resemble the paleomagnetic poles from younger strata in the region (Zhang et al., 2000, 2006), thus providing another argument in favor of its primary origin. It is close to, but distinguishable from, the key pole from the ~ 1.77 Ga Taihang dyke swarm (pole TD 1769 Ma in Fig. 5a) reported by Halls et al. (2000).

Table 1
Paleomagnetic results from the Xiong'er Group.

Site	n (N)	Dg	Ig	K	α_{95}	GPlat	GPlon	Dp/Dm	Ds	Is	Ks	α_{95}	SPlat	SPlon	Dp/Dm
Xushan Formation^a (34.0°N, 112.5°E)															
RY224	8	11.1	-21.7	53.2	7.7	43.5	277.4	4.3/8.1	13.8	-5.0	52.9	7.7	51.3	270.1	3.9/7.7
RY225	9	14.0	-27.8	136.9	4.4	39.4	274.9	2.6/4.8	17.6	-10.5	136.6	4.4	47.3	266.1	2.3/4.5
RY231	5	17.9	11.0	1267.4	2.2	57.1	258.3	1.1/2.2	17.3	15.4	1265.6	2.2	59.4	257.2	1.2/2.3
Ry243	5	193.3	1.8	103.2	7.6	-52.9	90.1	3.8/7.6	193.2	-3.2	103.6	7.6	-55.3	88.8	3.8/7.6
Mean on sample level	27	13.8	-14.1	22.4	6.0				15.6	-1.6	42.8	4.4			
Mean on site level	(4)	14.1	-10.1	20.2	21	48.4	271.1	A₉₅=11.2	15.5	0.8	50.0	13.1	53.4	265.9	A₉₅=7.0
Majiahe Formation (34.0°N, 112.5°E)															
RY208	8	213.7	-4.1	22.0	12.1	-45.2	60.6	6.1/12.1	213.4	-1.0	21.9	12.1	-44.2	62.4	6.1/12.1
RY211	8	15.1	-22.3	412.9	2.7	42.2	272.3	1.5/2.9	16.7	-13.7	416.8	2.7	46.1	268.2	1.4/2.8
RY2123	10	13.8	0.1	22.2	10.5	53.7	268.8	5.3/10.5	13.4	8.5	22.2	10.5	57.8	266.8	5.3/10.6
RY214	7	20.4	-15.1	206.9	4.2	44.1	263.8	2.2/4.3	21.4	-7.8	206.5	4.2	47.0	260.2	2.1/4.2
RY2156	9	22.9	19.0	59.6	6.7	57.9	246.2	3.6/7.0	21.4	22.0	59.7	6.7	60.1	246.6	3.7/7.1
RY217	9	14.2	5.8	18.9	12.1	56.2	266.4	6.1/12.1	13.0	12.6	19.0	12.1	59.9	266.1	6.3/12.3
RY218	4	13.4	-28.6	86.2	10.0	39.1	275.7	6.0/11.0	16.4	-22.1	86.2	10.0	41.9	270.7	5.6/10.6
RY219	6	15.7	-21.8	42.5	10.4	42.3	271.5	5.8/11.0	18.0	-14.6	42.3	10.4	45.2	266.7	5.5/10.7
RY220	6	18.4	-27.8	380.1	3.4	38.2	269.7	2.0/3.7	20.5	-20.1	376.5	3.5	41.5	265.1	1.9/3.7
RY221	9	19.5	-27.4	219.4	3.5	38.0	268.3	2.1/3.8	21.5	-19.7	219.0	3.5	41.4	263.8	1.9/3.7
Mean on sample level	76	18.9	-9.3	15.1	4.3				19.5	-3.3	17.1	4.1			
Mean on site level	(10)	18.8	-11.6	20.0	11.1	46.2	265.1	A₉₅=6.5	19.6	-5.5	24.2	10.0	48.8	262.0	A₉₅=5.9
Overall Xiong'er Group mean on site level (sample location: 34.0°N, 112.5°E)															
	(14)	17.4	-11.2	21.4	8.8	46.9	266.7	A₉₅=5.1	18.4	-3.7	28.5	7.6	50.2	263.0	A₉₅=4.5

n, number of samples demagnetized; *N*, number of sites; Dg/Ig, declination/inclination in the geographic coordinates; Ds/Is, declination/inclination in the stratigraphic coordinates; *K*, Fisher precision parameter for direction; α_{95} /A₉₅, radius of circle of 95% confidence about the direction/pole. GPlat/GPlon, latitude/longitude of VGP in the geographic coordinates; SPlat/SPlon, latitude/longitude of VGP in the stratigraphic coordinates; Dp/Dm, semi-axes of elliptical error around the pole at a probability of 95%.

^a Pass a reversals test: mean angle = 6.6° < γ = 8.3° Class B (McFadden and McElhinny, 1990).

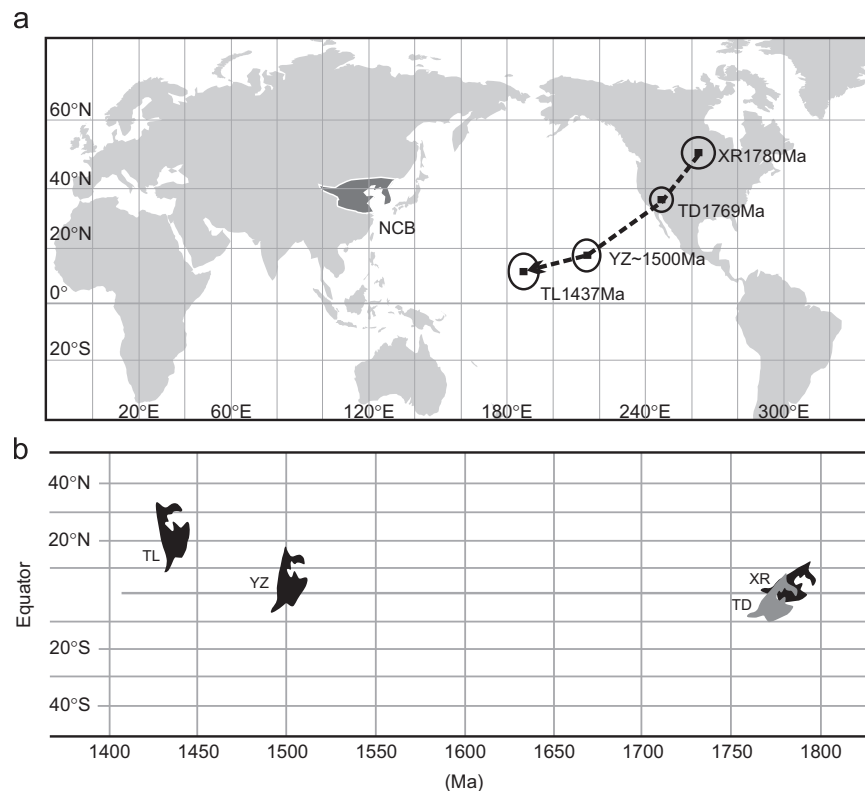


Fig. 5. (a) Selected high-quality Proterozoic paleomagnetic poles from the NCB plotted in present NCB coordinates. (b) Paleolatitudinal positions of the NCB between ~1.8 Ga and ~1.4 Ga, interpreted by the selected poles plotted in (Fig. 5a).

2.4. Paleomagnetic significance of recent geochronological progress on the Paleo-Mesoproterozoic successions in North China

The Jixian stratotype section in North China was previously thought to span the entire 1800–800 Ma interval with nearly

continuous deposition (see Zhang et al., 2006). Age constraints were largely limited to K–Ar results from glauconite or Ar/Ar results of chert layers, with only two U–Pb ages from the lower part of the succession (Lu and Li, 1991; Li H.K. et al., 1995). A more recent U–Pb SHRIMP age of 1379 ± 12 Ma from an ash bed

Table 2
Paleomagnetic poles selected for Nuna reconstruction.

Pole	Age (Ma)	Rock unit	Plat (°N)	Plon (°E)	A_{95} (Dm/Dp) (deg.)	Test ^a	References
North China Block (NCB)							
TL	1437 ± 21	Tieling Fm	11.6	187.1	8.1/4.9	F	Wu (2005)
YZ	1560–1440	Yangzhuang Fm	17.3	214.5	8.0/4.1	R, F	Wu et al. (2005)
TH	1769.1 ± 2.5	Taihang dyke swarm	36.0	247.0	2.8	C	Halls et al. (2000)
XR	~1780	Xiong'er Group	50.2	263.0	4.5	R	This study
Laurentia							
LG	1108 ± 1	Logan sills mean	49	220	4	C	Buchan et al. (2000)
AB	1141 ± 1	Abitibi dikes	43	209	13	C	Ernst and Buchan (1993)
SuD	1235+7/-3	Sudbury dikes	-3.0	192	3.0	C	Palmer et al. (1977)
MC	1267 ± 2	Mackenzie mean	04	190	5	C	Buchan and Halls (1990)
Zg	1382 ± 2	Zig-Zag Dal and intrusions	11.0	229	3	R	Evans and Mitchell (2011)
MN	1401 ± 6	McNamara Fm	-13.5	208.3	6.7	F	Elston et al. (2002)
MQ	~1420	Mistastin complex	-1.0	201.0	8.0	r	After Buchan et al. (2001)
LA	~1434	Laramie complex and Sherman granite	-7.0	215.0	4.0	r	After Buchan et al. (2001)
PC	1443 ± 7	Purcell lava	-23.6	215.6	4.8	F	Elston et al. (2002)
SN	1450 ± 14	Snowslip Fm	-24.9	210.2	3.5	F	Elston et al. (2002)
HL	~1450	Harp Lake complex	2.0	206.0	4.0	r	After Buchan et al. (2001)
MA	~1460	Michikamau anorthosite pluton	-2.0	218.0	5.0	C	After Buchan et al. (2001)
SF	1476 ± 16	St. Francois Mtns	-13.2	219.0	8.0/4.7	g, c, F	Meert and Stuckey (2002)
WC	ca. 1590	Western Channel	9	245	7	C	Irving et al. (1972, 2004) and Hamilton and Buchan (2010)
CD	1740+5/-4	Cleaver dikes	19	277	6	c, C	Irving et al. (2004)
MDB	~1880	Molson dyke, B component	27	219	4	C	Halls and Heaman (2000)
Slave/Laurentia							
Set	~1885	Seton mean	-6	260	4	c, r	Mitchell et al. (2010)
Kah	~1882	Kahochella mean	-12	285	7	r	Mitchell et al. (2010)
Doug	~1880	Douglas Peninsula Fm	-18	258	14	r	Irving and McClynn (1979)
St	~1875	Stark Fm	-15	215	5	r	Bingham and Evans (1976)
Toch	~1875	Tochatwi Fm	-18	216	11	F, r	Evans and Bingham (1976)
Pear	1870 ± 4	Pearson mean	-22	269	6	C, r	Mitchell et al. (2010)
Baltica							
MB	~1100	Mean for Baltica	1	208	16		Pesonen et al. (2003)
SA	1122 ± 7	Salla dike VGP	71	113	8.1	C	Salminen et al. (2009)
PJ	~1265	Post-Jotnian intrusives	04	158	4	C	Buchan et al. (2000)
LA	1452 ± 12	Lake Ladoga region	15.2	177.1	5.5	C	Lubnina et al. (2010)
AD	~1560	Aland Dolerite porphyry dykes	28.0	188.0	9.0	C	Buchan et al. (2001)
AQ	~1570	Aland Quartz porphyry dykes	12.0	182.0	7.0	C	Buchan et al. (2001)
SQ	~1630	Subjotnian quartz porphyry dykes	29.0	177.0	6.0		Pesonen et al. (2003)
SF	1770 ± 12	Shoksha Fm	39.7	221.1	5.5/2.9	R	Pisarevsky and Sokolov (2001)
Svec	~1880	Svecofennian Mean	41	233	5	Null	Pesonen et al. (2003)
Siberia							
Mil	~1025	Milkon Fm	-6.0	196	4.0	Null	After Pisarevsky and Natapov (2003)
Lin	~1070	Linok Fm	-15.2	256.2	7.5	F, R	Gallet et al. (2000)
Mal	~1070	Malgina Fm	-25.4	230.8	2.6	F, R, g	Gallet et al. (2000)
		<i>Malgina Fm, rotated to Anabar coordinates</i>	-15	250	3		
CD	1384 ± 2	Chieress dyke	4	258	9.0/5.0	(VGP)	Ernst and Buchan (2000)
OL	1473 ± 24	Olenëk mafic intrusions in Sololi Group	33.6	253.1	10.4	C	Wingate et al. (2009)
uAK	1863 ± 9	Upper Akitkan	-23	97	2	F	Didenko et al. (2009)
IaK	1878 ± 4	Lower Akitkan	-31	99	4	F	Didenko et al. (2009)
Australian Craton (in N Australia coordinate)^b							
LK	~1141	Lakeview Dolerite, N Australia	-10	131	17.5	Null	Tanaka and Idnurm (1994)
MM	~1210	Marnda Moorn mean pole, W Australia	-48	148	15.5	C, R	Evans (2009) and Pisarevsky et al. (2003)
		<i>Rotated to N Australia</i>	-33	165			
BDU	1589 ± 3	Balbirini Dolomite (upper), N Australia	-52	176.1	7.5	r	Idnurm (2000)
BDL	1613 ± 4	Balbirini Dolomite (lower), N Australia	-66.1	177.5	5.7	r	Idnurm (2000)
ED	1645	Emmerugga Dolomite, N Australia	-79.1	202.6	6.1	F	Idnurm et al. (1995)
TS	1650 ± 3	Tooganinie Formation, N Australia	-61	187	6	F	Idnurm et al. (1995)
WB	1709 ± 3	West Branch Volcanics, N Australia	-15.9	200.5	11.3	G	Idnurm (2000)
PC	~1725	Peters Creek Volcanics, N Australia	-26.0	221.0	4.8	g	Idnurm (2000)
EP	~1800	Elgee–Pentecost combined, N Australia	-5.4	211.8	4.5/2.3	F	Schmidt and Williams (2008) and Li (2000)
FF	~1800	Frere Formation, W Australia	-45.2	220.0	2.4/1.3	r, F	Williams et al. (2004)
		<i>After rotated to N Australia</i>	-8.3	209.3			
HP3	~1800	Hammersley Province overprint, W Australia	-35.3	211.9	3.0/3.0	F	Li et al. (2000)
		<i>After rotated to N Australia</i>	0.4	201.5			
India							
MA	1113 ± 7	Mahoba dikes	-38.7	49.5	18.3/10.8	(VGP)	Pradhan et al. (2012)
GW	~1798 ± 120	Gwalior traps	15.4	173.2	11.2/5.6	Null	Pradhan et al. (2010)
BA	~1880	Bastar Dykes and Cuddapah sills	31	330	12	R	Meert et al. (2011)

Table 2 (continued)

Pole	Age (Ma)	Rock unit	Plat (°N)	Plon (°E)	A ₉₅ (Dm/Dp) (deg.)	Test ^a	References
Amazonia							
NG	1418.5 ± 3.5	Nova Guarita mafic intrusives	−47.9	245.9	7.0	c	Bispo-Santos et al. (2012)
CS	1789 ± 7	Colider suite	−63.3	298.8	10.2	r	Bispo-Santos et al. (2008)

Fm, Formation; Plat/Plon, latitude/longitude of VGP; A₉₅, radius of circle of 95% confidence about the palaeopole. Other abbreviations are the same as in Table 1.

^a Field stability test abbreviations: F—fold test, c—inverse contact test, C—baked-contact test, g—conglomerate test, G—intraformational conglomerate test, R—reversals test, r—dual polarity. Note: capitalized symbols indicate primary magnetization, whereas lowercase symbols indicate merely ancient remanence relative to the geological feature of the test.

^b Poles from West Australia being rotated to North Australia using [−20, 135, 40]; poles from South Australia being rotated using [−18, 134, 51].

Table 3

Euler rotations for Nuna reconstruction.

Amazonia to Laurentia: (53, 293, 127), based on SAMBA geology (Johansson, 2009)
Baltica to Laurentia: (47.5, 1.5, 49), after Evans and Pisarevsky (2008)
Cathaysia to Laurentia: (57.5, 168, 177)
India to Laurentia: (56.0, 75.4, 123)
NCB to Laurentia: (45.7, 330.8, 33.4)
North Australia to Laurentia: (31.5, 098, 102.5) after Evans and Mitchell (2011) and Payne et al. (2009)
Mawson block to North Australia: South Australia to North Australia (−18, 134, 51), after Payne et al. (2009)
West Australia to North Australia (−20, 135, 40), after Li and Evans (2011)
Mawson block, E Antarctica to present Australia (−2, 38.9, 31.5), after Powell and Li (1994)
Siberia to Laurentia: Anabar block to Laurentia (78, 099, 147), after Evans and Mitchell (2011)
Aldan to Anabar before Devonian (60, 115, 25), after Evans (2009)
W Africa to Laurentia: (30, 266, 70.7), based on SAMBA geology (Johansson, 2009)
Laurentia absolute rotation (for use in Fig. 7 only): For 1.59 Ga reconstruction (0, 155, 81)
For 1.74 Ga reconstruction (0, 187, 71)

within the Xiamaling Formation (Su et al., 2008) dramatically changed that perspective, and constrained most of Jixian deposition to the interval of 1800–1400 Ma. Subsequently, more U–Pb ages on ash beds have confirmed the early Mesoproterozoic ages for the pre-Xiamaling strata: 1559 ± 12 Ma (SHRIMP U–Pb zircon) and 1560 ± 5 Ma (LA-MC-ICPMS U–Pb zircon) for the Gaoyuzhuang Formation (Li et al., 2010), and 1437 ± 21 Ma (SHRIMP U–Pb zircon) for the Tieling Formation (Su et al., 2010). The ca. 1560 Ma age for the Gaoyuzhuang Formation provides a maximum age constraint for the high-quality Yangzhuang Formation red-bed pole (Pei et al., 2006; Wu et al., 2005); the ca. 1437 Ma age for the Tieling Formation age can be directly applied to the paleomagnetic data from the limestone units of that formation (Wu, 2005) as well as the previously published data from that unit (see review in Zhang et al. (2006)). The age of the Yangzhuang Formation is herein estimated at ca. 1550–1500 Ma, based on its maximum constraint provided by the underlying Gaoyuzhuang Formation (1560 ± 5 Ma), and the minimum constraint provided by the 1437 ± 21 Ma Tieling Formation which is two formations above the Yangzhuang Formation.

The key poles from the Xiong'er Group (XR, with best estimated age of 1780 Ma) and Taihang dykes (TD, 1769 Ma), plus two others from the Yangzhuang (YZ, ~1500 Ma) and the Tieling (TL, 1437 Ma) formations in the Jixian section in North China, define a preliminary apparent polar wander path (APWP) for the NCB through the interval of ~1780–1440 Ma (Fig. 5a). These poles indicate that the NCB drifted from near the paleo-equator to low-latitude regions during this period (Fig. 5b), consistent

with the occurrence of paleoclimatic indicators such as redbeds, reefs and dolomites in these strata.

3. Reconstructing Nuna using paleomagnetic data

In the following discussion, we use the paleomagnetic method to determine the relative positions of continents by matching their APWPs (or fragments of APWPs), but at the same time consider geological arguments for possible past connections. Paleomagnetic data were selected using Van der Voo's (1990) 7-point criteria system and they are listed in Table 2, including each pole's age information, position and error parameters, most important field stability tests performed, and the original references. This data table includes new results from the NCB, and other newly published results for other continents. There is good data coverage for Laurentia, Baltica and the NCB for the interval of ~1.78–1.40 Ga. Australia has good data coverage for the 1.80–1.60 Ga interval. However, for the remaining cratons, the data are spread more sparsely.

Using the available high-quality paleomagnetic data (Table 2), we present in Fig. 6 a reconstruction of Nuna that includes all the world's major cratons. The tight Laurentia–Siberia–Baltica fit proposed by Evans and Mitchell (2011) can be conjoined to the SAMBA fit of Baltica with Amazon and West Africa (Johansson, 2009), with an additional constraint provided by the new 1.42-Ga paleomagnetic pole from Amazon (Bispo-Santos et al., 2012). On the other side of Nuna, the Australia–Mawsonland–Laurentia connection of Payne et al. (2009) is modified to include additional intracontinental deformation following that of Li and Evans (2011), in a “proto-SWEAT” connection similar to that shown in outline form by Evans and Mitchell (2011), except that we now have ca. 1.8–1.6 Ga paleomagnetic data supporting such a connection (Fig. 6a and b, and discussions below).

Herein we add two other cratons to a quantified Nuna reconstruction: India is placed according to a ca. 1.8-Ga pole from its Bundelkhand massif (Pradhan et al., 2010), and the NCB is positioned by superimposing its four selected poles between 1.78 Ga and ~1.44 Ga atop coeval poles from the combined cratonic assemblage as described above (Fig. 6). Our paleomagnetic interpretation supports the geological idea that the present south margin of the NCB represented an active continental margin in Nuna and likely faced an open ocean, whilst its north margin was connected to a large landmass (Zhao et al., 2011). Zhao et al. (2002, 2011) and Zhao G. et al. (2004) placed the NCB adjacent to India on the basis of similarities between their Archean to Paleoproterozoic basement terranes, and our paleomagnetic reconstruction supports such a connection for Nuna time, but pre-1.8 Ga paleomagnetic data from both cratons are still lacking. Recent geochronological work has dated mafic sills in northern NCB at ~1.33 Ga (Zhang et al., 2009, in press), which

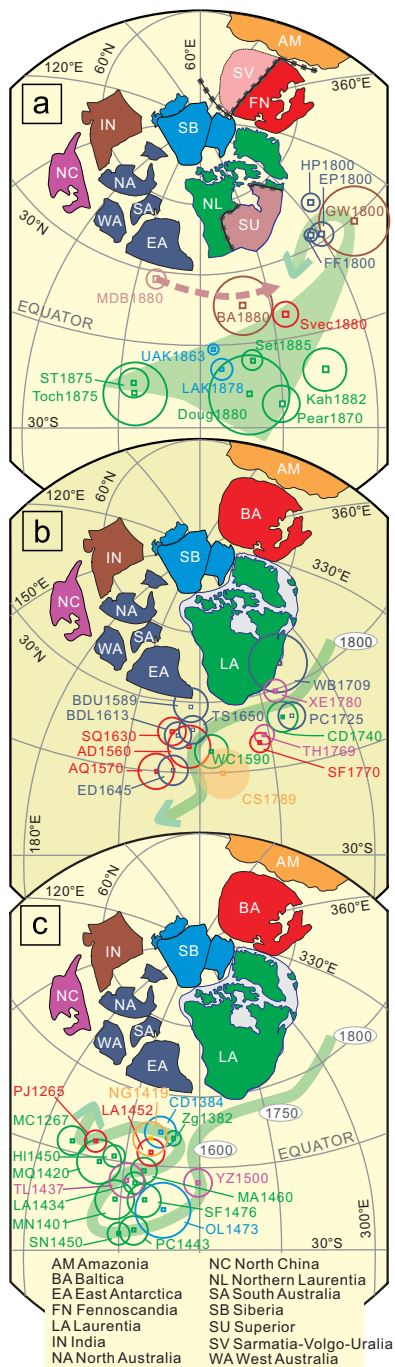


Fig. 6. Selected paleomagnetic poles for the reconstruction of Nuna, all in present North American coordinates, according to Euler rotation parameters given in Table 3. Cratons and their poles are matched in color, and ages following pole abbreviations are in Ma. For more details see Table 2. (a) Paleomagnetic poles between ~ 1.88 and ~ 1.80 Ga, showing broad convergence (light-green swath) of poles from the Slave craton of Laurentia, Siberia, Baltica, India and Australia, which suggests that these blocks might commence to join together at ~ 1.80 Ga. Arrow points toward the position of younger poles. (b) Poles between ~ 1.78 Ga and ~ 1.60 Ga from Australian cratons, Laurentia, Baltica and NCB define a common APWP of Nuna (green curve); arrow points toward the position of younger poles. Pole CS1789 from Amazonia is out of the map region, indicating that this craton might not have joined the union until after ~ 1.79 Ga. (c) Paleomagnetic poles for ~ 1.50 – 1.265 Ga from the NCB, Siberia, Laurentia, Baltica and Amazonia against the common APWP (green curve) that is defined by all poles between 1.8 Ga and 1.265 Ga, indicating common motion to at least ~ 1.38 Ga. Arrow points toward the position of younger ($< \sim 1.2$ Ga) poles from Laurentia and Baltica.

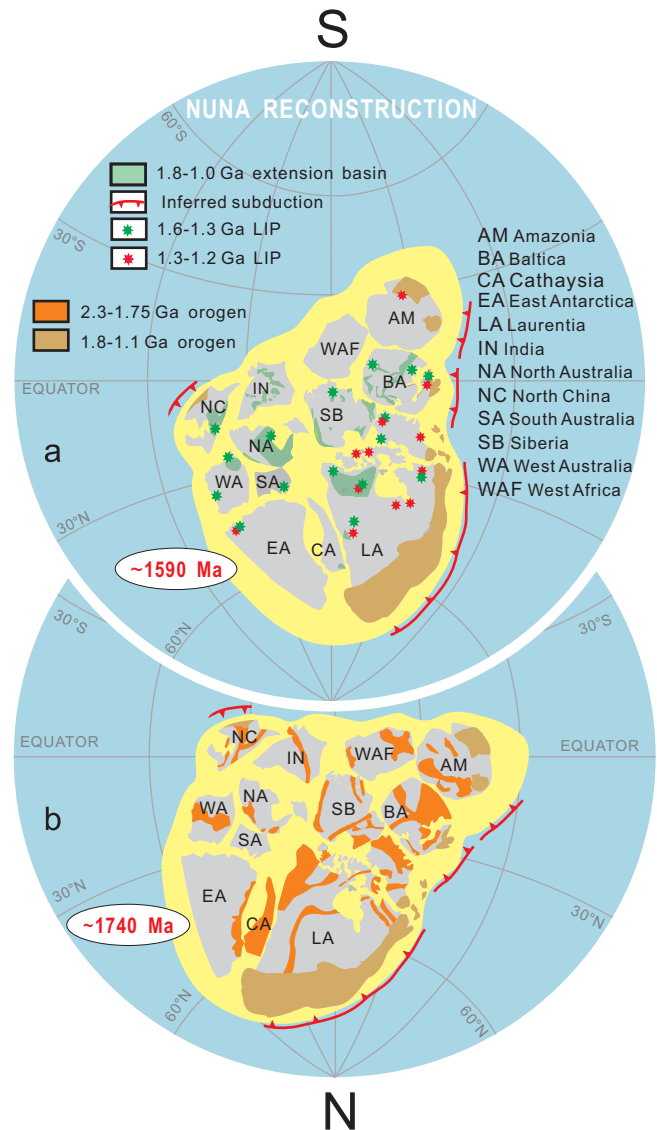


Fig. 7. Configuration and paleogeographic position of the supercontinent Nuna. (a) ~ 1.59 Ga, when large igneous provinces and extensional basins were extensively developed; (b) ~ 1.74 Ga, soon after assembly of Nuna. Paleomagnetic poles from Laurentia (WC1590 and CD1740 in Table 2) were used to plot the paleolatitude of the supercontinent. Placing Laurentia in northern hemisphere was based on the likely westward trade-wind direction interpreted by Hoffman and Grotzinger (1993) from the ~ 1.95 – 1.86 Ga geological records in the Slave Craton.

match well with the Derim-Derim sills in northern Australia (Sweet et al., 1999), and our reconstruction similarly aligns the extensive Paleoproterozoic sedimentary basins in both regions (Fig. 7a). Those basins contain an excellent record of early eukaryotic biological development (Javaux et al., 2001), and their geochemistry signals have been interpreted to represent global oceanic chemistry (Planavsky et al., 2011; Shen et al., 2003). Our reconstruction implies that such successions developed interior to the Nuna supercontinent, perhaps marginal to isolated oceanic basins, like the modern Black Sea. Marginal or isolated seas should be enriched in sulfur species from riverine input, relative to the open ocean. Because Planavsky et al. (2011) found a ferrous rather than euxinic signal of iron speciation in such basins, their argument for a ferrous global ocean is strengthened by our proposed paleogeography.

Although some continental blocks plotted in Fig. 6 have no high quality paleomagnetic poles older than 1.78 Ga, the ~ 1.88 –

1.80 Ga poles from India, Australia, Baltica, Siberia and the Slave block of Laurentia broadly define a convergent swath through that interval (Fig. 6a). This indicates that these blocks might have commenced to connect to each other earlier, as a single plate representing the accretionary core of the nascent supercontinent. The Superior craton joined the assembly at ca. 1.81 Ga (St-Onge et al., 2009), and Wyoming craton accreted even later, at ca. 1.75 Ga (Dahl et al., 1999). The 1.79-Ga pole from Amazonia also does not support this configuration (Fig. 6b) and suggests that Amazonia might have joined Nuna later, also, perhaps as part of a single plate with Volgo–Sarmatia that docked against Fennoscandia at ca. 1.75 Ga (Bogdanova et al., 2008; Elming et al., 2001).

The 1770-Ma poles from Baltica and North China, as reconstructed, imply a small APWP oscillation in geon 17, which we did not illustrate for the sake of simplicity (Fig. 6b). The 1645 Ma ED pole from northern Australia is shown atop younger poles from Baltica, but it lies at the apex of a prominent oscillation in the McArthur Basin APWP for Australia (Idnurm, 2000). If northern Australia was part of Nuna, and if that oscillation is real, then it merely has not been sampled yet by other cratons, which generally have a poor geon-16 paleomagnetic record. The paleopole from the ~1590 Ma Gawler Range Volcanics has recently been suggested to be a late Paleozoic remagnetization (Schmidt and Clark, 2011), and has therefore been removed from the data table here. The considerable scatter in the geon-14 poles from Laurentia is independent of our reconstruction.

Despite these anomalies, with our reconstruction that encompasses almost all major continents, all selected high-quality poles for the time interval of 1.8–1.4 Ga fall on a common APWP (Fig. 6b and c), whereas poles of >1.8 Ga from different continents or cratons diverge with increasing ages (Fig. 6a). These data suggest that Nuna was likely assembled by ca. 1.8 Ga (Fig. 7b), as speculated on geological grounds (Hoffman, 1997; Rogers and Santosh, 2002; Zhao et al., 2002; Zhao G. et al., 2004). In addition, we place the Cathaysia block of south China as an extension of western Laurentia, as proposed by Li and co-workers (Li Z.X. et al., 1995; Li et al., 2008b). West Africa is devoid of Mesoproterozoic paleomagnetic data, but we follow Johansson (2009) in proposing a long-lived connection of that block to Baltica and Amazon. The only large cratons missing from our model are Congo–São Francisco and Kalahari, which lack reliable data from the interval 1.8–1.3 Ga, the Yangtze craton of south China, and Tarim, both of which lack extensive pre-Neoproterozoic exposures and may themselves be collages of much smaller earlier continental fragments.

Widespread 1.6–1.2 Ga large igneous events across the supercontinent (Fig. 7a) may signify early extension related to the breakup of Nuna. However, as discussed earlier in this paper, paleomagnetic data appear to support a coherent Nuna until ca. 1.40 Ga. Paleomagnetic poles younger than ca. 1.3–1.2 Ga (Table 2), when rotated into the coordinates of our reconstructed Nuna configuration, diverge from each other; this implies Nuna's breakup at that time, coincident with emplacement of numerous late Mesoproterozoic large igneous provinces (cf. Ernst et al., 2008; Evans and Mitchell, 2011). At the moment, paleomagnetic poles are lacking for many continents for the time interval of 1.4–1.2 Ga (Table 2), and we are therefore yet unable to determine more precisely exactly when did Nuna broke apart. However, if the widespread 1.28–1.26 Ga large igneous events are linked to the supercontinent disaggregation (Evans and Mitchell, 2011), then the prolonged 1.6–1.2 Ga LIP events in the lead-up of Nuna fragmentation is not dissimilar to the protracted breakup process of Rodinia, which lasted over 200 Myr from ca. 850 Ma initial rifting (Li et al., 2008a; Li et al., 2011), to 720–650 Ma major fragmentation (Li and Evans, 2011) and ca. 600 Ma final dispersal (Cawood and Pisarevsky, 2006).

4. Conclusions

We report here new paleomagnetic results from the ~1780 Ma Xiong'er Group in NCB, which have yielded a high quality paleomagnetic pole at 50.2°N, 263.0°E ($N=14$, $A_{95}=4.5^\circ$). Together with three other high quality paleomagnetic poles from the NCB, with ages of ~1769 Ma, ~1500 Ma and ~1437 Ma, they define a ca. 1780–1400 Ma APWP for the NCB, depicting Equatorial to low-latitude paleogeographic positions that are in good agreement with the climate indicators in the strata.

A review of all available global paleomagnetic data enabled us to reconstruct, for the first time, a near-complete global-scale supercontinent Nuna (also known as Columbia) that formed by ca. 1.75 Ga, and lasted till at least ca. 1.4 Ga (Figs. 6 and 7). Our paleomagnetism-based global reconstruction is in agreement with previously proposed, geologically based models, including the SAMBA connection between Baltica, Amazonia and Western Africa (Johansson, 2009), the Nuna core connection between Laurentia, Baltica and Siberia (Evans and Mitchell, 2011), the proto-SWEAT connection between Laurentia, Mawson block and Australian blocks (Goodge et al., 2008; Payne et al., 2009) and the NCB–India connection (Zhao et al., 2011). In addition, our reconstruction for the first time, quantitatively merges them into a single and coherent supercontinent.

Our Nuna reconstruction, constrained by both our new results and an updated global paleomagnetic dataset, is also consistent with key geological features including the ca. 1.8 Ga orogenic belts leading to the assembly of Nuna (Fig. 7b) and Mesoproterozoic global intraplate extensional basins and large igneous province (LIP) record possibly related to the breakup of Nuna (Fig. 7a).

The breakup of Nuna may have commenced after ca. 1.4 Ga, but available paleomagnetic data are not yet complete enough to allow a more precise depiction of Nuna's fragmentation.

Acknowledgments

This work was jointly supported by the 973 Program (Grant No. 2011CB808800), NSFC projects 40921062, 40974035, 40032010B and 40830316, SinoProbe Program and ARC discovery Grant (DP0770228). This is contribution 197 from the ARC Centre of Excellence for Core to Crust Fluid Systems, and TIGER publication 423. We thank Professor Paul F. Hoffman and an anonymous reviewer for their constructive reviews.

References

- Bingham, D.K., Evans, M.E., 1976. Paleomagnetism of the Great Slave Supergroup, Northwest Territories, Canada: the Stark Formation. *Can. J. Earth Sci.* 13, 563–578.
- Bispo-Santos, F., D'Agrella-Filho, M.S., Trindade, R.I.F., Elming, S.-Å., Janikian, L., Vasconcelos, P.M., Perillo, B.M., Pacca, I.I.G., da Silva, J.A., Barros, M.A.S., 2012. Tectonic implications of the 1419 Ma Nova Guarita mafic intrusives paleomagnetic pole (Amazonian Craton) on the longevity of Nuna. *Precambrian Res.* 196–197, 1–22.
- Bispo-Santos, F., D'Agrella-Filho, M.S., Pacca, I.I.G., Janikian, L., Trindade, R.I.F., Elming, S.-Å., Silva, J.A., Barros, M.A.S., Pinho, F.E.C., 2008. Columbia revisited: paleomagnetic results from the 1790 Ma Colider volcanics (SW Amazonian Craton, Brazil). *Precambrian Res.* 164, 40–49.
- Bogdanova, S.V., Bingen, B., Gorbatschev, R., Kheraskova, T.N., Kozlov, V.I., Puchkov, V.N., Volozh, Y.A., 2008. The East European Craton (Baltica) before and during the assembly of Rodinia. *Precambrian Res.* 160, 23–45.
- Buchan, K.L., Ernst, R.E., Hamilton, M.A., Mertenan, S., Pesonen, L.J., Elming, S.-Å., 2001. Rodinia: the evidence from integrated palaeomagnetism and U–Pb geochronology. *Precambrian Res.* 110, 9–32.
- Buchan, K.L., Halls, H.C., 1990. Paleomagnetism of Proterozoic mafic dyke swarms of the Canadian Shield. In: Parker, A.J., Rickwood, P.C., Tucker, D.H. (Eds.), *Mafic Dykes and Emplacement Mechanisms*. Balkema, Rotterdam, pp. 209–230.
- Buchan, K.L., Mertenan, S., Park, R.G., Pesonen, L.J., Elming, S.-Å., Abrahamsen, N., Bylund, G., 2000. Comparing the drift of Laurentia and Baltica in the

- Proterozoic: the importance of key palaeomagnetic poles. *Tectonophysics* 319, 167–198.
- Cawood, P.A., Pisarevsky, S.A., 2006. Was Baltica right-way-up or upside-down in the Neoproterozoic? *J. Geol. Soc. London* 163, 753–759.
- Dahl, P.S., Holm, D.K., Gardner, E.T., Hubacher, F.A., Folland, K.A., 1999. New constraints on the timing of Early Proterozoic tectonism in the Black Hills (South Dakota), with implications for the docking of the Wyoming Province with Laurentia. *Geol. Soc. Am. Bull.* 111, 1335–1349.
- Didenko, A.N., Vodovozov, V.Y., Pisarevsky, S.A., Gladkochub, D.P., Donskaya, T.V., Mazukabzov, A.M., Stanevich, A.M., Bibikova, E.V., Kirnozova, T.I., 2009. Palaeomagnetism and U–Pb dates of the Palaeoproterozoic Akitkan Group (South Siberia) and implications for pre-Neoproterozoic tectonics. In: Reddy, S.M., Mazumder, R., Evans, D.A.D., Collins, A.S. (Eds.), *Palaeoproterozoic Supercontinents and Global Evolution*. Geological Society Special Publications, London, pp. 145–163.
- Dunlop, D.J., 2002. Theory and application of the Day plot (Mrs/Ms versus Hcr/Hc) 1. Theoretical curves and tests using titanomagnetite data. *J. Geophys. Res.* 107, 2056–2077, <http://dx.doi.org/10.1029/2001JB000486>.
- Elming, S.-Å., Mikhailova, N.P., Kravchenko, S., 2001. Palaeomagnetism of Proterozoic rocks from the Ukrainian Shield: new tectonic reconstructions of the Ukrainian and Fennoscandian shields. *Tectonophysics* 339, 19–38.
- Elston, D.P., Enkin, R.J., Baker, J., Kisilevsky, D.K., 2002. Tightening the Belt: paleomagnetic-stratigraphic constraints on deposition, correlation, and deformation of the Middle Proterozoic (ca. 1.4 Ga) Belt–Purcell Supergroup, United States and Canada. *Geol. Soc. Am. Bull.* 114, 619–638.
- Ernst, R.E., Buchan, K.L., 1993. Palaeomagnetism of the Abitibi dyke swarm, southern Superior Province, and implications for the Logan Loop. *Can. J. Earth Sci.* 30, 1886–1897.
- Ernst, R.E., Buchan, K.L., 2000. Integrated Palaeomagnetism and U–Pb geochronology of mafic dikes of the Eastern Anabar Shield. *J. Geol.* 108, 381.
- Ernst, R.E., Wingate, M.T.D., Buchan, K.L., Li, Z.X., 2008. Global record of 1600–700 Ma Large Igneous Provinces (LIPs) with implications for the reconstruction of the proposed Nuna (Columbia) and Rodinia supercontinents. *Precambrian Res.* 160, 159–178.
- Evans, D.A.D., 2009. The Palaeomagnetically Viable, Long-lived and All-inclusive Rodinia Supercontinent Reconstruction, vol. 327. Geological Society Special Publications, London (pp. 371–404).
- Evans, M.E., Bingham, D.K., 1976. Palaeomagnetism of the Great Slave Supergroup, Northwest Territories, Canada: the Tochatwi Formation. *Can. J. Earth Sci.* 13, 555–562.
- Evans, D.A.D., Mitchell, R.N., 2011. Assembly and breakup of the core of Paleoproterozoic–Mesoproterozoic supercontinent Nuna. *Geology* 39, 443–446.
- Evans, D.A.D., Pisarevsky, S.A., 2008. Plate tectonics on early Earth? Weighing the paleomagnetic evidence. In: Condie, K.C., Pease, V. (Eds.), *When Did Plate Tectonics Begin on Planet Earth?*. Geological Society of America Special Papers, pp. 249–263.
- Fisher, R., 1953. Dispersion on a sphere. *Proc. R. Soc. London Ser. A: Math. Phys. Sci.* 217, 295–305.
- Gallet, Y., Pavlov, V.E., Semikhatov, M.A., Petrov, P.Y., 2000. Late Mesoproterozoic magnetostratigraphic results from Siberia: paleogeographic implications and magnetic field behavior. *J. Geophys. Res.* 105, 16481–16499.
- Goode, J.W., Vervoort, J.D., Fanning, C.M., Brecke, D.M., Farmer, G.L., Williams, I.S., Myrow, P.M., DePaolo, D.J., 2008. A positive test of east Antarctica–Laurentia juxtaposition within the Rodinia supercontinent. *Science* 321, 235–240.
- Halls, H.C., Heaman, L.M., 2000. The paleomagnetic significance of new U–Pb age data from the Molson dyke swarm, Cauchon Lake area, Manitoba. *Can. J. Earth Sci.* 37, 957–966.
- Halls, H.C., Li, J., Davis, D., Hou, G., Zhang, B., Qian, X., 2000. A precisely dated Proterozoic palaeomagnetic pole from the North China craton, and its relevance to palaeocontinental reconstruction. *Geophys. J. Int.* 143, 185–203.
- Hamilton, M.A., Buchan, K.L., 2010. U–Pb geochronology of the Western Channel Diabase, northwestern Laurentia: implications for a large 1.59 Ga magmatic province, Laurentia's APWP and paleocontinental reconstructions of Laurentia, Baltica and Gawler craton of southern Australia. *Precambrian Res.* 183, 463–473.
- He, Y., Zhao, G., Sun, M., Xia, X., 2009. SHRIMP and LA-ICP-MS zircon geochronology of the Xiong'er volcanic rocks: implications for the Paleo-Mesoproterozoic evolution of the southern margin of the North China Craton. *Precambrian Res.* 168, 213–222.
- Hoffman, P.F., 1997. Tectonic genealogy of North America. In: Van der Pluijm, B.A., Marshak, S. (Eds.), *Earth Structure: An Introduction to Structural Geology and Tectonics*. McGraw-Hill, New York, pp. 459–464.
- Hoffman, P.F., Grotzinger, J.P., 1993. Orographic precipitation, erosional unloading, and tectonic style. *Geology* 21, 195–198.
- Idnurm, M., 2000. Towards a high resolution Late Palaeoproterozoic–earliest Mesoproterozoic apparent polar wander path for northern Australia. *Aust. J. Earth Sci.* 47, 405–429.
- Idnurm, M., Giddings, J.W., 1995. Paleoproterozoic–Neoproterozoic North America–Australia link: new evidence from paleomagnetism. *Geology* 23, 149–152.
- Idnurm, M., Giddings, J.W., Plumb, K.A., 1995. Apparent polar wander and reversal stratigraphy of the Palaeo-Mesoproterozoic southeastern McArthur Basin, Australia. *Precambrian Res.* 72, 1–41.
- Irving, E., Baker, J., Hamilton, M., Wynne, P.J., 2004. Early Proterozoic geomagnetic field in western Laurentia: implications for paleolatitudes, local rotations and stratigraphy. *Precambrian Res.* 129, 251–270.
- Irving, E., Donaldson, J.A., Park, J.K., 1972. Paleomagnetism of the Western Channel Diabase and associated rocks, Northwest Territories. *Can. J. Earth Sci.* 9, 960–971.
- Irving, E., McGlynn, J.C., 1979. Palaeomagnetism in the Coronation Geosyncline and arrangement of continents in the middle Proterozoic. *Geophys. J. R. Astron. Soc.* 58, 309–336.
- Javaux, E.J., Knoll, A.H., Walter, M.R., 2001. Morphological and ecological complexity in early eukaryotic ecosystems. *Nature* 412, 66–69.
- Johansson, Å., 2009. Baltica, Amazonia and the SAMBA connection—1000 million years of neighbourhood during the Proterozoic? *Precambrian Res.* 175, 221–234.
- Kirschvink, J.L., 1980. The least-squares line and plane and the analysis of palaeomagnetic data. *Geophys. J. R. Astron. Soc.* 62, 699–718.
- Li, H.K., Li, H.M., Lu, S.N., 1995. Grain zircon U–Pb ages for volcanic rocks from Tuanshanzi Formation of Changcheng system and their geological implications. *Geochimica* 24, 43–48.
- Li, H.K., Zhu, S.X., Xiang, Z.Q., Su, W.B., Lu, S.N., Zhou, H.Y., Geng, J.Z., Li, S., Yang, F.J., 2010. Zircon U–Pb dating on tuff bed from Gaoyuzhuang Formation in Yanqing, Beijing: further constraints on the new subdivision of the Mesoproterozoic stratigraphy in the northern North China Craton. *Acta Petrol. Sin.* 26, 2131–2140.
- Li, W.X., Li, X.H., Li, Z.X., 2011. Ca. 850 Ma bimodal volcanic rocks in northeastern Jiangxi Province, south China: initial extension during the breakup of Rodinia? *Am. J. Sci.* 310, 951–980.
- Li, Z.X., 2000. Palaeomagnetic evidence for unification of the North and West Australian cratons by ca. 1.7 Ga: new results from the Kimberley Basin of northwestern Australia. *Geophys. J. Int.* 142, 173–180.
- Li, Z.X., Bogdanova, S.V., Collins, A.S., Davidson, A., De Waele, B., Ernst, R.E., Fitzsimons, I.C.W., Fuck, R.A., Gladkochub, D.P., Jacobs, J., Karlstrom, K.E., Lu, S., Natapov, L.M., Pease, V., Pisarevsky, S.A., Thrane, K., Vernikovsky, V., 2008a. Assembly, configuration, and break-up history of Rodinia: a synthesis. *Precambrian Res.* 160, 179–210.
- Li, Z.X., Evans, D.A.D., 2011. Late Neoproterozoic 40° intraplate rotation within Australia allows for a tighter-fitting and longer-lasting Rodinia. *Geology* 39, 39–42.
- Li, Z.X., Guo, W., Powell, C.M., 2000. Timing and Genesis of Hamersley BIF-hosted Iron Deposits: A New Palaeomagnetic Interpretation. MERIWA Project M242. Minerals and Energy Research Institute of Western Australia Report no. 199, pp. 216.
- Li, Z.X., Li, X.H., Li, W.X., Ding, S.J., 2008b. Was Cathaysia part of Proterozoic Laurentia? New data from Hainan Island, south China. *Terra Nova* 20, 154–164.
- Li, Z.X., Zhang, L., Powell, C.M., 1995. South China in Rodinia: part of the missing link between Australia–East Antarctica and Laurentia? *Geology* 23, 407–410.
- Lu, S., Li, H., 1991. A precise U–Pb single zircon age determination for the volcanics of Dahongyu Formation, Changcheng system in Jixian. *Bull. Chin. Acad. Geol. Sci.* 22, 137–146.
- Lubnina, N.V., Mertenanen, S., Söderlund, U., Bogdanova, S., Vasilieva, T.I., Frank-Kamenetsky, D., 2010. A new key pole for the East European Craton at 1452 Ma: palaeomagnetic and geochronological constraints from mafic rocks in the Lake Ladoga region (Russian Karelia). *Precambrian Res.* 183, 442–462.
- McFadden, P.L., McElhinny, M.W., 1990. Classification of the reversal test in palaeomagnetism. *Geophys. J. Int.* 103, 725–729.
- Meert, J.G., Pandit, M.K., Pradhan, V.R., Kamenov, G., 2011. Preliminary report on the paleomagnetism of 1.88 Ga dykes from the Bastar and Dharwar cratons, Peninsular India. *Gondwana Res.* 20, 335–343.
- Meert, J.G., Stuckey, W., 2002. Revisiting the paleomagnetism of the 1.476 Ga St. Francois Mountains igneous province, Missouri. *Tectonics* 21, 1007.
- Mitchell, R.N., Hoffman, P.F., Evans, D.A.D., 2010. Coronation loop resurrected: oscillatory apparent polar wander of Orosirian (2.05–1.8 Ga) paleomagnetic poles from Slave craton. *Precambrian Res.* 179, 121–134.
- Nance, R.D., Worsley, T.R., Moody, J.B., 1988. The supercontinent cycle. *Sci. Am.* 259, 72–79.
- Palmer, H.C., Merz, B.A., Hayatsu, A., 1977. The Sudbury dikes of the Grenville Front region: paleomagnetism, petrochemistry, and K–Ar age studies. *Can. J. Earth Sci.* 14, 1867–1887.
- Payne, J.L., Hand, M., Barovich, K.M., Reid, A., Evans, D.A.D., 2009. Correlations and reconstruction models for the 2500–1500 Ma evolution of the Mawson Continent. In: Reddy, S.M., Mazumder, R., Evans, D.A.D., Collins, A.S. (Eds.), *Palaeoproterozoic Supercontinents and Global Evolution*. Geological Society Special Publications, London, pp. 319–355.
- Pei, J., Yang, Z., Zhao, Y., 2006. A Mesoproterozoic paleomagnetic pole from the Yangzhuang Formation, North China and its tectonic implications. *Precambrian Res.* 151, 1–13.
- Pesonen, L.J., Elming, S.-Å., Mertenanen, S., Pisarevsky, S., D'Agrella-Filho, M.S., Meert, J.G., Schmidt, P.W., Abrahamsen, N., Bylund, G., 2003. Palaeomagnetic configuration of continents during the Proterozoic. *Tectonophysics* 375, 289–324.
- Pisarevsky, S.A., Natapov, L.M., 2003. Siberia and Rodinia. *Tectonophysics* 375, 221–245.
- Pisarevsky, S.A., Sokolov, S.J., 2001. The magnetostratigraphy and a 1780 Ma palaeomagnetic pole from the red sandstones of the Vazhinka River section, Karelia, Russia. *Geophys. J. Int.* 146, 531–538.
- Pisarevsky, S.A., Wingate, M.T.D., Powell, C.M., Johnson, S., Evans, D.A.D., 2003. Models of Rodinia Assembly and Fragmentation, vol. 206. Geological Society Special Publications, London (pp. 35–55).

- Planavsky, N.J., McGoldrick, P., Scott, C.T., Li, C., Reinhard, C.T., Kelly, A.E., Chu, X., Bekker, A., Love, G.D., Lyons, T.W., 2011. Widespread iron-rich conditions in the mid-Proterozoic ocean. *Nature* 477, 448–451.
- Powell, C.McA., Li, Z.X., 1994. Reconstructions of the Panthalassan margin of Gondwanaland. In: Veevers, J.J., Powell, C.McA. (Eds.), *Permian-Triassic Pangean Basins and Foldbelts Along the Panthalassan Margin of Gondwanaland*, 184. Geological Society of America Memoir, pp. 5–9.
- Pradhan, V.R., Meert, J.G., Pandit, M.K., Kamenov, G., Gregory, L.C., Malone, S.J., 2010. India's changing place in global Proterozoic reconstructions: a review of geochronologic constraints and paleomagnetic poles from the Dharwar, Bundelkhand and Marwar cratons. *J. Geodyn.* 50, 224–242.
- Pradhan, V.R., Meert, J.G., Pandit, M.K., Kamenov, G., Mondal, M.E.A., 2012. Paleomagnetic and geochronological studies of the mafic dyke swarms of Bundelkhand craton, central India: implications for the tectonic evolution and paleogeographic reconstructions. *Precambrian Res.* 198–199, 51–76.
- Ren, F.G., Li, H.M., Yin, Y.J., Li, S.B., Ding, S.Y., Chen, Z.H., 2000. The upper chronological limit of the Xiong'er Group's volcanic rock series, and its geological significance. *Prog. Precambrian Res.* 23, 140–146. (in Chinese with English abstract).
- Rogers, J.J.W., Santosh, M., 2002. Configuration of Columbia, a Mesoproterozoic Supercontinent. *Gondwana Res.* 5, 5–22.
- Salminen, J., Pesonen, L.J., Reimold, W.U., Donadini, F., Gibson, R.L., 2009. Paleomagnetic and rock magnetic study of the Vredefort impact structure and the Johannesburg Dome, Kaapvaal Craton, South Africa—implications for the apparent polar wander path of the Kaapvaal Craton during the Mesoproterozoic. *Precambrian Res.* 168, 167–184.
- Schmidt, P.W., Williams, G.E., 2008. Palaeomagnetism of red beds from the Kimberley Group, Western Australia: implications for the palaeogeography of the 1.8 Ga King Leopold glaciation. *Precambrian Res.* 167, 267–280.
- Schmidt, P.W., Clark, D.A., 2011. Magnetic characteristics of the Hiltaba Suite Granitoids and Volcanics: late Devonian overprinting and related thermal history of the Gawler Craton. *Aust. J. Earth Sci.* 58, 361–374.
- Shen, Y., Knoll, A.H., Walter, M.R., 2003. Evidence for low sulphate and anoxia in a mid-Proterozoic marine basin. *Nature* 423, 632–635.
- St-Onge, M.R., Van Gool, J.A.M., Garde, A.A., Scott, D.J., 2009. Correlation of Archaean and Palaeoproterozoic units between northeastern Canada and western Greenland: constraining the pre-collisional upper plate accretionary history of the Trans-Hudson orogen. In: Cawood, P.A., Kröner, A. (Eds.), *Earth Accretionary Systems in Space and Time*. Geological Society of London Special Publications, pp. 193–235.
- Su, W., Li, H., Huff, W., Etensohn, F., Zhang, S., Zhou, H., Wan, Y., 2010. SHRIMP U–Pb dating for a K-bentonite bed in the Tieling Formation, North China. *Chin. Sci. Bull.* 55, 3312–3323.
- Su, W., Zhang, S., Huff, W.D., Li, H., Etensohn, F.R., Chen, X., Yang, H., Han, Y., Song, B., Santosh, M., 2008. SHRIMP U–Pb ages of K-bentonite beds in the Xiamaling Formation: implications for revised subdivision of the Meso- to Neoproterozoic history of the North China Craton. *Gondwana Res.* 14, 543–553.
- Sweet, I.P., Brakel, A.T., Rawlings, D.J., Haines, P.W., Plumb, K.A., Wygralak, A.S., 1999. Mount Marumba, Northern Territory—1:250,000 Geological Map Series Sheet SD 53-6 With Explanatory Notes, 2nd ed. Australian Geological Survey Organisation and Northern Territory Geological Survey. (National Science Mapping Accord).
- Tanaka, H., Idnurm, M., 1994. Palaeomagnetism of Proterozoic mafic intrusions and host rocks of the Mount Isa Inlier, Australia: revisited. *Precambrian Res.* 69, 241–258.
- Van der Voo, R., 1990. The reliability of paleomagnetic data. *Tectonophysics* 184, 1–9.
- Veevers, J.J., 2004. Gondwanaland from 650–500 Ma assembly through 320 Ma merger in Pangea to 185–100 Ma breakup: supercontinental tectonics via stratigraphy and radiometric dating. *Earth-Sci. Rev.* 68, 1–132.
- Wang, Y., Fan, W., Zhang, Y., Guo, F., Zhang, H., Peng, T., 2004. Geochemical, $^{40}\text{Ar}/^{39}\text{Ar}$ geochronological and Sr–Nd isotopic constraints on the origin of Paleoproterozoic mafic dikes from the southern Taihang Mountains and implications for the ca. 1800 Ma event of the North China Craton. *Precambrian Res.* 135, 55–77.
- Williams, G.E., Schmidt, P.W., Clark, D.A., 2004. Palaeomagnetism of iron-formation from the late Palaeoproterozoic Frere Formation, Earahedy Basin, Western Australia: palaeogeographic and tectonic implications. *Precambrian Res.* 128, 367–383.
- Wingate, M.T.D., Pisarevsky, S.A., Gladkochub, D.P., Donskaya, T.V., Konstantinov, K.M., Mazukabzov, A.M., Stanevich, A.M., 2009. Geochronology and paleomagnetism of mafic igneous rocks in the Olenek Uplift, northern Siberia: implications for Mesoproterozoic supercontinents and paleogeography. *Precambrian Res.* 170, 256–266.
- Wu, H., 2005. New Paleomagnetic Results from Mesoproterozoic Successions in Jixian Area, North China Block, and Their Implications for Paleocontinental Reconstructions. *China University of Geosciences, Beijing*, p. 133.
- Wu, H., Zhang, S., Li, Z.X., Li, H., Dong, J., 2005. New paleomagnetic results from the Yangzhuang Formation of the Jixian System, North China, and tectonic implications. *Chin. Sci. Bull.* 50, 1483–1489.
- Zhang, S., Li, Z.X., Wu, H., 2006. New Precambrian palaeomagnetic constraints on the position of the North China Block in Rodinia. *Precambrian Res.* 144, 213–238.
- Zhang, S., Li, Z.X., Wu, H., Wang, H., 2000. New paleomagnetic results from the Neoproterozoic successions in southern North China Block and paleogeographic implications. *Sci. China Ser. D: Earth Sci.* 43, 233–244.
- Zhang, S.H., Zhao, Y., Santosh, M. Mid-Mesoproterozoic bimodal magmatic rocks in the northern North China Craton: implications for magmatism related to breakup of the Columbia supercontinent. *Precambrian Res.*, <http://dx.doi.org/10.1016/j.precamres.2011.06.00>, in press.
- Zhang, S.H., Zhao, Y., Yang, Z.Y., He, Z.F., Wu, H., 2009. The 1.35 Ga diabase sills from the northern North China Craton: implications for breakup of the Columbia (Nuna) supercontinent. *Earth. Planet. Sci. Lett.* 288, 588–600.
- Zhao, G., Cawood, P.A., Wilde, S.A., Sun, M., 2002. Review of global 2.1–1.8 Ga orogens: implications for a pre-Rodinia supercontinent. *Earth-Sci. Rev.* 59, 125–162.
- Zhao, G., Li, S., Sun, M., Wilde, S.A., 2011. Assembly, accretion, and break-up of the Palaeo-Mesoproterozoic Columbia supercontinent: record in the North China Craton revisited. *Int. Geol. Rev.* 53, 1331–1356.
- Zhao, G., Sun, M., Wilde, S.A., Li, S., 2004. A Paleo-Mesoproterozoic supercontinent: assembly, growth and breakup. *Earth-Sci. Rev.* 67, 91–123.
- Zhao, T.P., Zhai, M.G., Xia, B., Li, H.M., Zhang, Y.X., Wan, Y.S., 2004. Zircon U–Pb SHRIMP dating for the volcanic rocks of the Xiong'er Group: constrains on the initial formation age of the cover of the North China Craton. *Chin. Sci. Bull.* 49, 2495–2502.